



# **HIF-1 $\alpha$ Deletion in the Endothelium, but Not in the Epithelium, Protects From Radiation-Induced Enteritis**

Aurore Toullec, Valérie Buard, Emilie Rannou, Georges Tarlet, Olivier Guipaud, Sylvie Robine, M Luisa Iruela-Arispe, Agnès François, Fabien Milliat, M. Luisa Iruela-Arispe

## **► To cite this version:**

Aurore Toullec, Valérie Buard, Emilie Rannou, Georges Tarlet, Olivier Guipaud, et al.. HIF-1 $\alpha$  Deletion in the Endothelium, but Not in the Epithelium, Protects From Radiation-Induced Enteritis. Cellular and Molecular Gastroenterology and Hepatology, 2018, 5 (1), pp.15-30. 10.1016/j.jcmgh.2017.08.001 . hal-02902657

**HAL Id: hal-02902657**

**<https://hal.science/hal-02902657>**

Submitted on 20 Jul 2020

**HAL** is a multi-disciplinary open access archive for the deposit and dissemination of scientific research documents, whether they are published or not. The documents may come from teaching and research institutions in France or abroad, or from public or private research centers.

L'archive ouverte pluridisciplinaire **HAL**, est destinée au dépôt et à la diffusion de documents scientifiques de niveau recherche, publiés ou non, émanant des établissements d'enseignement et de recherche français ou étrangers, des laboratoires publics ou privés.



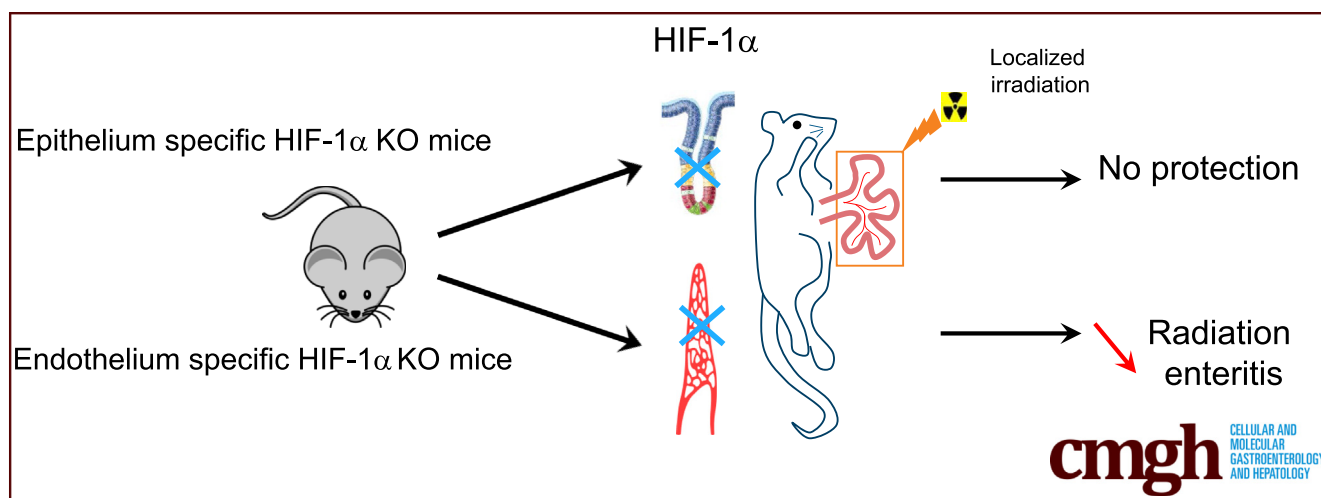
Distributed under a Creative Commons Attribution - NonCommercial - NoDerivatives 4.0 International License

## ORIGINAL RESEARCH

HIF-1 $\alpha$  Deletion in the Endothelium, but Not in the Epithelium, Protects From Radiation-Induced Enteritis

Aurore Toullec,<sup>1</sup> Valérie Buard,<sup>1</sup> Emilie Rannou,<sup>1,2</sup> Georges Tarlet,<sup>1</sup> Olivier Guipaud,<sup>1</sup> Sylvie Robine,<sup>3</sup> M. Luisa Iruela-Arispe,<sup>2</sup> Agnès François,<sup>1</sup> and Fabien Milliat<sup>1</sup>

<sup>1</sup>Research Laboratory of Radiobiology and Radiopathology, Institute for Radiological Protection and Nuclear Safety, Fontenay-aux-Roses, France; <sup>2</sup>Department of Molecular, Cell, and Developmental Biology, University of California, Los Angeles, California; and the <sup>3</sup>Curie Institute, Paris, France



## SUMMARY

This study examines the cell type-specific impact of hypoxia-inducible factor-1 $\alpha$  activation in disease. The authors show that endothelial hypoxia-inducible factor-1 $\alpha$  deletion confers resistance to radiation-induced enteritis, but similar deletion in intestinal epithelium does not. These results suggest new functions of endothelial hypoxia-inducible factor-1 $\alpha$ -signaling pathways as mediators of mucosal inflammatory processes.

**BACKGROUND & AIMS:** Radiation therapy in the pelvic area is associated with side effects that impact the quality of life of cancer survivors. Interestingly, the gastrointestinal tract is able to adapt to significant changes in oxygen availability, suggesting that mechanisms related to hypoxia sensing help preserve tissue integrity in this organ. However, hypoxia-inducible factor (HIF)-dependent responses to radiation-induced gut toxicity are unknown. Radiation-induced intestinal toxicity is a complex process involving multiple cellular compartments. Here, we investigated whether epithelial or endothelial tissue-specific HIF-1 $\alpha$  deletion could affect acute intestinal response to radiation.

**METHODS:** Using constitutive and inducible epithelial or endothelial tissue-specific HIF-1 $\alpha$  deletion, we evaluated the

consequences of epithelial or endothelial HIF-1 $\alpha$  deletion on radiation-induced enteritis after localized irradiation. Survival, radiation-induced tissue injury, molecular inflammatory profile, tissue hypoxia, and vascular injury were monitored.

**RESULTS:** Surprisingly, epithelium-specific HIF-1 $\alpha$  deletion does not alter radiation-induced intestinal injury. However, irradiated VECad-Cre<sup>+/+</sup>-HIF-1 $\alpha$ <sup>FL/FL</sup> mice present with lower radiation-induced damage, showed a preserved vasculature, reduced hypoxia, and reduced proinflammatory response compared with irradiated HIF-1 $\alpha$ <sup>FL/FL</sup> mice.

**CONCLUSIONS:** We demonstrate *in vivo* that HIF-1 $\alpha$  impacts radiation-induced enteritis and that this role differs according to the targeted cell type. Our work provides a new role for HIF-1 $\alpha$  and endothelium-dependent mechanisms driving inflammatory processes in gut mucosae. Results presented show that effects on normal tissues have to be taken into account in approaches aiming to modulate hypoxia or hypoxia-related molecular mechanisms. (*Cell Mol Gastroenterol Hepatol* 2018;5:15–30; <http://dx.doi.org/10.1016/j.jcmgh.2017.08.001>)

**Keywords:** HIF-1 $\alpha$ ; Endothelium; Radiation.

See editorial on page 61.

**R**adiation therapy is a powerful treatment for patients with cancer. However, radiation is also associated with side effects caused by the exposure of healthy tissues adjacent to the radiation field.<sup>1,2</sup> For many years, the pathogenesis of radiation enteropathy has been exclusively explained by the severity of the depletion of progenitor epithelial cells based in crypts. Today, the contemporary vision of radiation enteropathy pathogenesis is integrated and involves multiple cell compartments that interact in a complex sequence of events following the radiation insult.<sup>3,4</sup> Thus, the immune system, enteric nervous system, macrovascular and microvascular systems, mesenchymal and epithelial cells, and even gut microbiome can contribute to the initiation and progression of radiation-induced intestinal injury. Moreover, the pathophysiology of radiation enteropathy is a multifaceted process involving activation of the coagulation cascade, inflammation, epithelial regeneration, accumulation of granulation tissue, and matrix deposition and remodeling.<sup>4,5</sup>

Exposure of normal tissues to high-dose ionizing radiation, including the intestinal wall, induces capillary loss and provokes phenotypic endothelial cell alteration with the acquisition of a proinflammatory, prothrombotic, and antifibrinolytic phenotype.<sup>6</sup> Microvascular injury is a prominent feature of both early mucosal ulceration and delayed intestinal wall fibrosis. Endothelial cell depletion can directly impact tissue oxygen content and consequently lead to cellular adaptation to changes in oxygen. At the molecular level, cellular adaptation to hypoxia is mainly driven by hypoxia-inducible factors (HIFs), which are inactive when oxygen is abundant and activated under hypoxic conditions.<sup>7</sup> The HIF-1 transcription factor is a heterodimer of 2 subunits: the highly oxygen-regulated  $\alpha$  subunit (HIF-1 $\alpha$ ) and a constitutively expressed  $\beta$  subunit (HIF-1 $\beta$ ). In normoxia, HIF-1 $\alpha$  protein is hydroxylated by prolyl hydroxylases. Hydroxylated HIF-1 $\alpha$  forms a complex with von Hippel-Lindau protein, which results in ubiquitination and subsequent proteasomal degradation. Under hypoxic conditions, prolyl hydroxylase activity is inhibited and HIF-1 $\alpha$  accumulates, translocates to the nucleus, and activates the expression of target genes by binding to hypoxia-responsive elements.

Prolyl hydroxylases are key regulators of intestinal barrier function<sup>8</sup> and relationships between hypoxia and inflammation and interdependence between hypoxic and immune responses have been documented.<sup>9,10</sup> Inflamed lesions often become hypoxic and hypoxia impacts a broad panel of inflammatory response genes, in part by HIF-1-dependent mechanisms. Overexpression of HIF-1 was observed in high-grade radiation-induced proctitis, suggesting that HIF-1 can be a key player in the pathogenesis of radiation-induced rectum injury.<sup>11</sup> In preclinical models of total body or global abdominal irradiation, pharmacologic prolyl hydroxylase inhibitor increases HIF activity, which protects against radiation-induced gut toxicity by an HIF-2- but not HIF-1-dependent mechanism.<sup>12</sup> Moreover, using HIF-1 and HIF-2 lox-stop-lox mice crossed with Tie-2-Cre transgenic mice to activate HIF-1 or HIF-2 in the


endothelium, Taniguchi et al<sup>12</sup> showed that endothelial-specific expression of either HIF-1 or HIF-2 was not sufficient to protect against gastrointestinal syndrome after 18-Gy abdominal irradiation. Interestingly, conditional epithelial activation for HIF-2 but not for HIF-1 protects against radiation gastrointestinal toxicity after 18-Gy abdominal irradiation. These results showed that epithelial, but not endothelial, HIF-2 mediates the radioprotective effect and that HIF-1 is not involved. These results highlight the complexity of hypoxia-associated mechanisms in the intestinal response to stress, but the role of hypoxia-dependent molecular signals in radiation-induced intestinal inflammation remains unclear. Here, we investigated whether epithelial- or endothelial-specific HIF-1 $\alpha$  genetic deletion affects acute exposure of the gut to localized radiation.

## Materials and Methods

### Mouse Models and Genotyping

All animal experimental procedures were approved by the ethics committee of the Institute for Radiological Protection and Nuclear Safety (protocol number P13-18). The conditional tissue-specific HIF-1 $\alpha$  deletion was generated by crossing transgenic mice expressing Cre recombinase with HIF-1 $\alpha$  floxed mice (B6.129-Hif1 $\alpha^{tm3Rsj}$ ) strain from The Jackson Laboratory (Sacramento, CA). These mice possess loxP sites on either side of exon 2<sup>13</sup> (Figure 1A). The following mice were used for this study: VE-cadherin-Cre (VECad-Cre) mice,<sup>14</sup> VECad-CreER<sup>T2</sup> mice,<sup>15</sup> Villin-Cre mice,<sup>16</sup> Villin-CreER<sup>T2</sup> mice,<sup>17</sup> and ROSA26R LacZ reporter (ROSA) mice (The Jackson Laboratory). Crossing of these lines was used to obtain the following mice: VECad-Cre<sup>+/+</sup>/ROSA<sup>+/+</sup>, Villin-Cre<sup>+/+</sup>/ROSA<sup>+/+</sup>, VECad-CreER<sup>T2</sup>+/ROSA<sup>+/+</sup>, Villin-CreER<sup>T2</sup>+/ROSA<sup>+/+</sup>, HIF-1 $\alpha^{FL/FL}$ VECad-Cre<sup>+/+</sup>, HIF-1 $\alpha^{FL/FL}$ VECad-CreER<sup>T2</sup>+/ROSA<sup>+/+</sup>, HIF-1 $\alpha^{FL/FL}$ Villin-Cre<sup>+/+</sup>, and HIF-1 $\alpha^{FL/FL}$ Villin-CreER<sup>T2</sup>+/ROSA<sup>+/+</sup> (Figure 1B). Genotyping of transgenic animals was performed by polymerase chain reaction (PCR) on tail DNA to determine the genotype (Figure 1C). Primer sequences for genotyping were as follows: Primers GGTGCTGGTGTCACAAATGT (forward) and GGGCAGTACTGGAAAGATGG (reverse) were used to detect a 345-bp product for the floxed HIF-1 $\alpha$  allele and a 295-bp product for the wild-type allele, primers GCAGGCAGCTCACAAAGGAACAAT (forward) TGTCCTTGCTGAGTGACAGTGGAA (reverse) were used to amplify a 550-bp product for the wild-type allele and a 310-bp product for the Cre transgene in VECad-Cre mice, and

**Abbreviations used in this paper:** EndoMT, endothelial-to-mesenchymal transition; HIF, hypoxia-inducible factor; HIF-1 $\alpha^{FL/FL}$ , HIF-1 $\alpha$  floxed mice; HIMEC, human intestinal microvascular endothelial cells; HUVEC, human umbilical vein endothelial cells; IL, interleukin; PAI-1, plasminogen activator inhibitor type-1; PCR, polymerase chain reaction; ROSA, ROSA26R LacZ reporter mice; Sham-IR, sham irradiation; TBI, total body irradiation; VECad-Cre, VE-cadherin-Cre mice.

 Most current article

© 2018 The Authors. Published by Elsevier Inc. on behalf of the AGA Institute. This is an open access article under the CC BY-NC-ND license (<http://creativecommons.org/licenses/by-nc-nd/4.0/>).

2352-345X

<http://dx.doi.org/10.1016/j.jcmgh.2017.08.001>

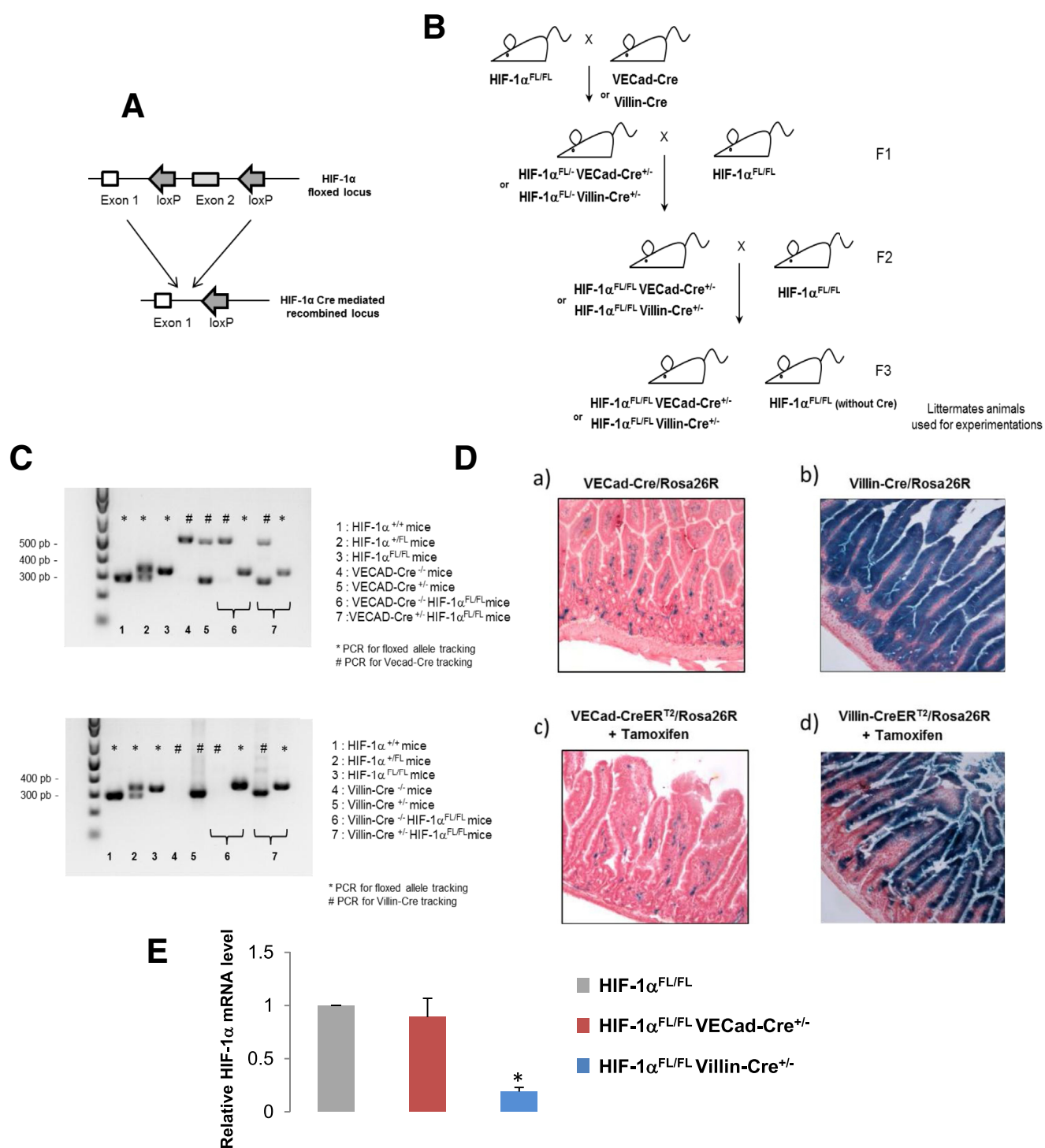


**Figure 1. (A) Molecular targeting strategy for HIF-1 $\alpha$  deletion. (B) Global breeding scheme for producing transgenic mice for experiments. For inducible models using VECad-CreER $^{T2}$  or Villin-CreER $^{T2}$ , the same breeding protocol was used and mice were treated with tamoxifen to produce recombination events. (C) Genotype identification from DNA tail by PCR to discriminate each mouse genotype. (D) Specific recombination events in endothelium or in epithelium in intestinal tissue. Recombination events were checked using ROSA26R reporter mice. LacZ staining of gut from VECad-Cre/Rosa26R mice, Villin-Cre/Rosa26R, and VECad-CreER $^{T2}$ /Rosa26R Villin-CreER $^{T2}$ /Rosa26R. (E) Relative HIF-1 $\alpha$  mRNA expression in intestinal tissue from HIF-1 $\alpha^{FL/FL}$  mice, HIF-1 $\alpha^{FL/FL}$  VECad-Cre $^{+/+}$  mice, and HIF-1 $\alpha^{FL/FL}$  Villin-Cre $^{+/+}$  mice. Results are mean  $\pm$  standard error of the mean with 12 mice per group. \* $P < .05$  versus HIF-1 $\alpha^{FL/FL}$  group.**



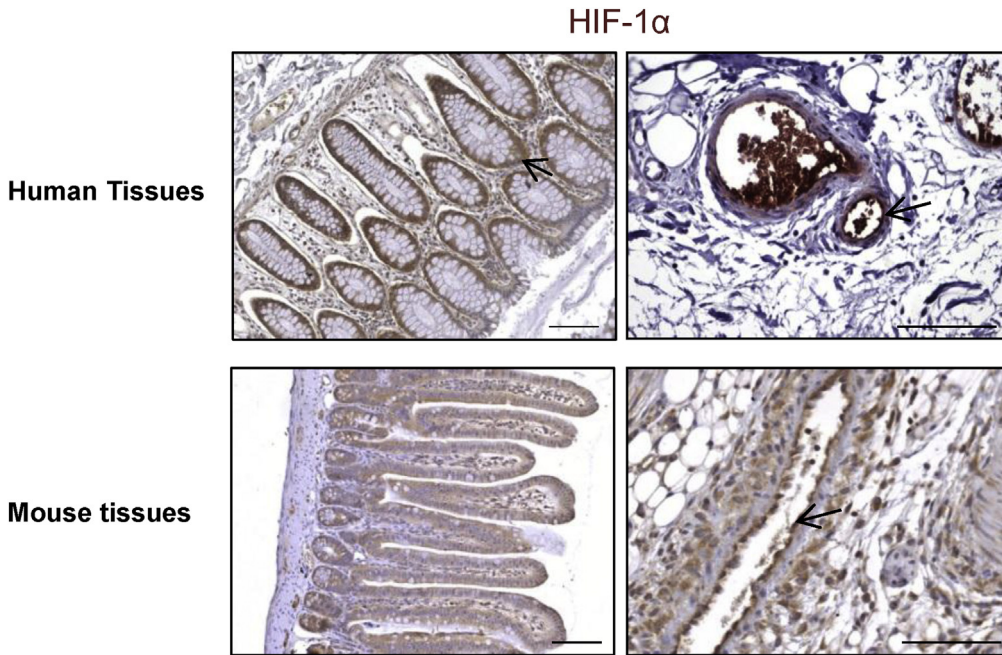


**Figure 2.** HIF-1 $\alpha$  expression in human and mouse gastrointestinal tract. Representative immunostaining of HIF-1 $\alpha$  shows expression in both epithelium and endothelium.

primers CAAGCCTGGCTCGACGGCC (forward) and CGCGAA-CATCTTCAGGTTCT (reverse) were used to detect a 300-bp product for the Cre transgene allele in both Villin-Cre and Villin-CreER<sup>T2</sup> mice. Presence or absence of the ROSA26 fragment was determined using 3 primers: R1: 5'-AAAGTCGCTCTGAGTTGTTAT -3' forward, R2: 5'-GCGAA-GAGTTTGTCTCAACC-3' reverse, and R3: 5'-GGAGCGGGA-GAAATGGATATG -3' reverse. R1 and R2 detected the ROSA26 fragment (603 bp), whereas R1 and R3 detected the endogenous locus (therefore absence of ROSA26 fragment) (340 bp). Activation of CreER<sup>T2</sup> recombinase was induced by daily intraperitoneal injections of 2 mg tamoxifen (diluted in 10% EtOH in sunflower oil) for 5 days. Irradiations occurred 1 week after the first injection, a time point at which we checked that CreER<sup>T2</sup> recombinase was functional.

### Animal Experimental Procedures

Radiation enteropathy was induced by exposure of an intestinal segment to 19 Gy of radiation as previously described.<sup>18</sup> Briefly, mice were anesthetized with isoflurane and, after laparotomy, a 3-cm-long intestinal segment was exteriorized and exposed to a single dose of 19 Gy of gamma irradiation (<sup>60</sup>Co source, dose rate 0.8 Gy/min). Sham-irradiation (Sham-IR) was performed by maintaining the intestinal segment exteriorized without radiation exposure. After radiation exposure or Sham-IR, the exposed segment was returned to the abdominal cavity and peritoneum/abdominal muscles and skin were separately closed with interrupted sutures. For the radiation-induced gastrointestinal syndrome model, 13 Gy total body irradiation (TBI) was performed using a <sup>60</sup>Co source (dose rate 0.8 Gy/min) or an Elekta Synergy Platform (Elekta SAS France, Boulogne, France) delivering 4 MV X-rays at 2.5 Gy/min. Tissue hypoxia was assessed using a Hypoxyprobe-1 kit (Chemicon, Millipore, France). Pimonidazole hydrochloride

was given at a dose of 60 mg/kg in 0.9% saline via retro-orbital injection 45 minutes before euthanasia. For positive control, 5 C57/BL6J mice underwent mesenteric vascular ligation to induce local hypoxia of part of the small intestine for 15 minutes before euthanasia. Vascular integrity was assessed using fluorescently (fluorescein isothiocyanate) labeled *Griffonia (Bandeiraea) simplicifolia* lectin 1 (Sigma, Saint-Quentin Fallavier, France). BS1-lectin fluorescein isothiocyanate was given at a dose of 2.5 mg/kg in 0.9% saline via retro-orbital injection 45 minutes before euthanasia.

### Histology and Immunohistochemistry

For  $\beta$ -galactosidase staining, intestinal tissues were embedded with Tissue-Tek OCT (Sakura Finetek, France) mounting medium and frozen in isopentane cooled by liquid nitrogen. Assays were performed using the  $\beta$ -Gal staining kit (Invitrogen LifeTechnologies, France) according to the manufacturer's instructions. Slides were counterstained with nuclear fast red (Sigma, Saint-Quentin Fallavier, France) according to the manufacturer's instructions.

To perform global analyses of the irradiated tissues, histology and immunohistochemistry were performed on different groups of animals. For routine histology analysis, intestines were fixed in 4% formaldehyde solution and embedded in paraffin. Longitudinal sections (5  $\mu$ m) were stained with hematoxylin-eosin-saffron. Radiation injury score was previously described in detail.<sup>18</sup>

Crypts surviving irradiation were identified based on histologic appearance (ie, undilated and possessing at least 10 well-stained epithelial cells and 1 Paneth cell). Surviving crypts were counted using the histolab image analysis software (Microvision Instruments, France), over a total tissue length of between 3000 and 5000  $\mu$ m, and related to 1000  $\mu$ m.

For immunohistochemistry experiments, intestinal tissues were embedded in paraffin and staining was

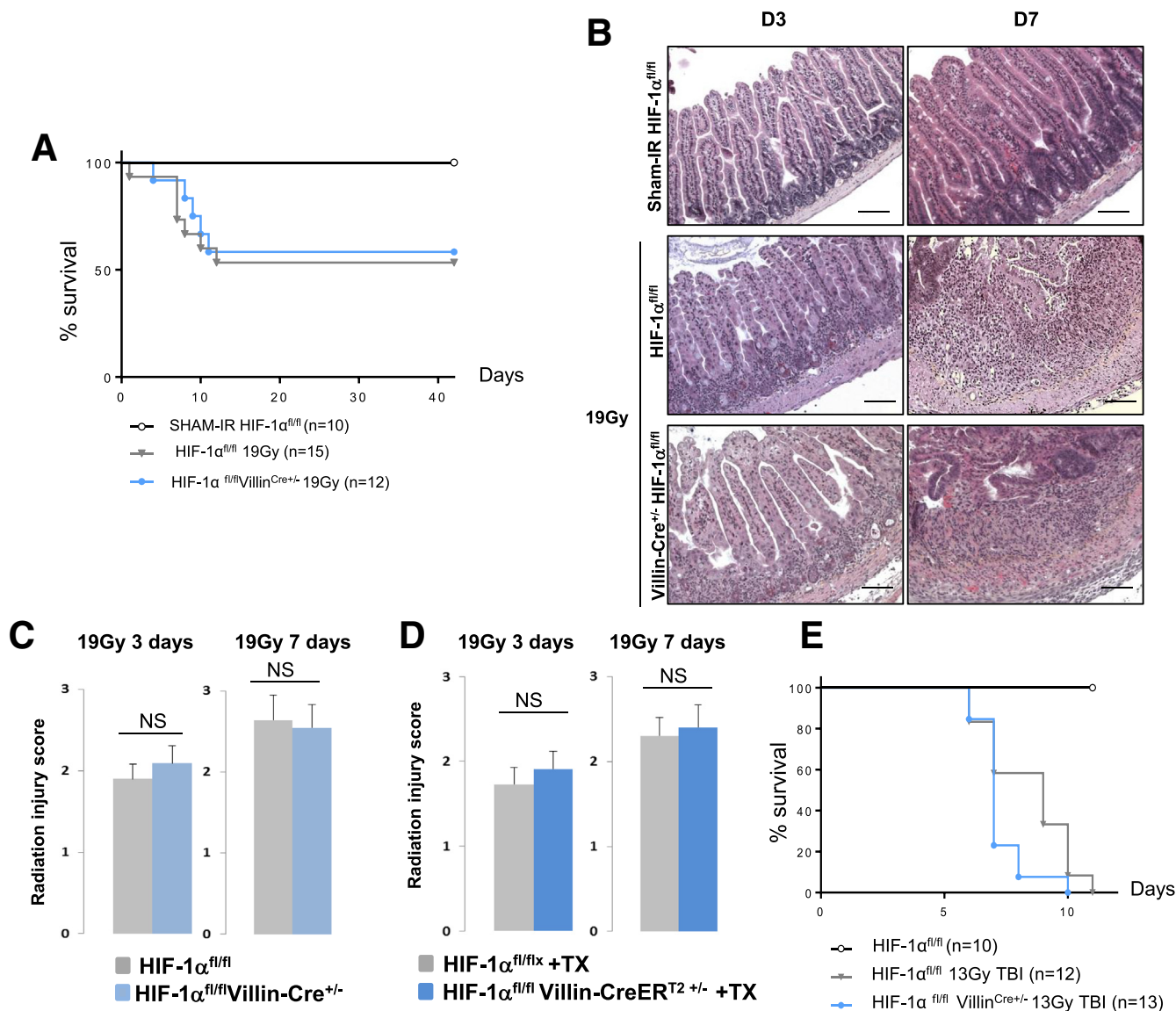
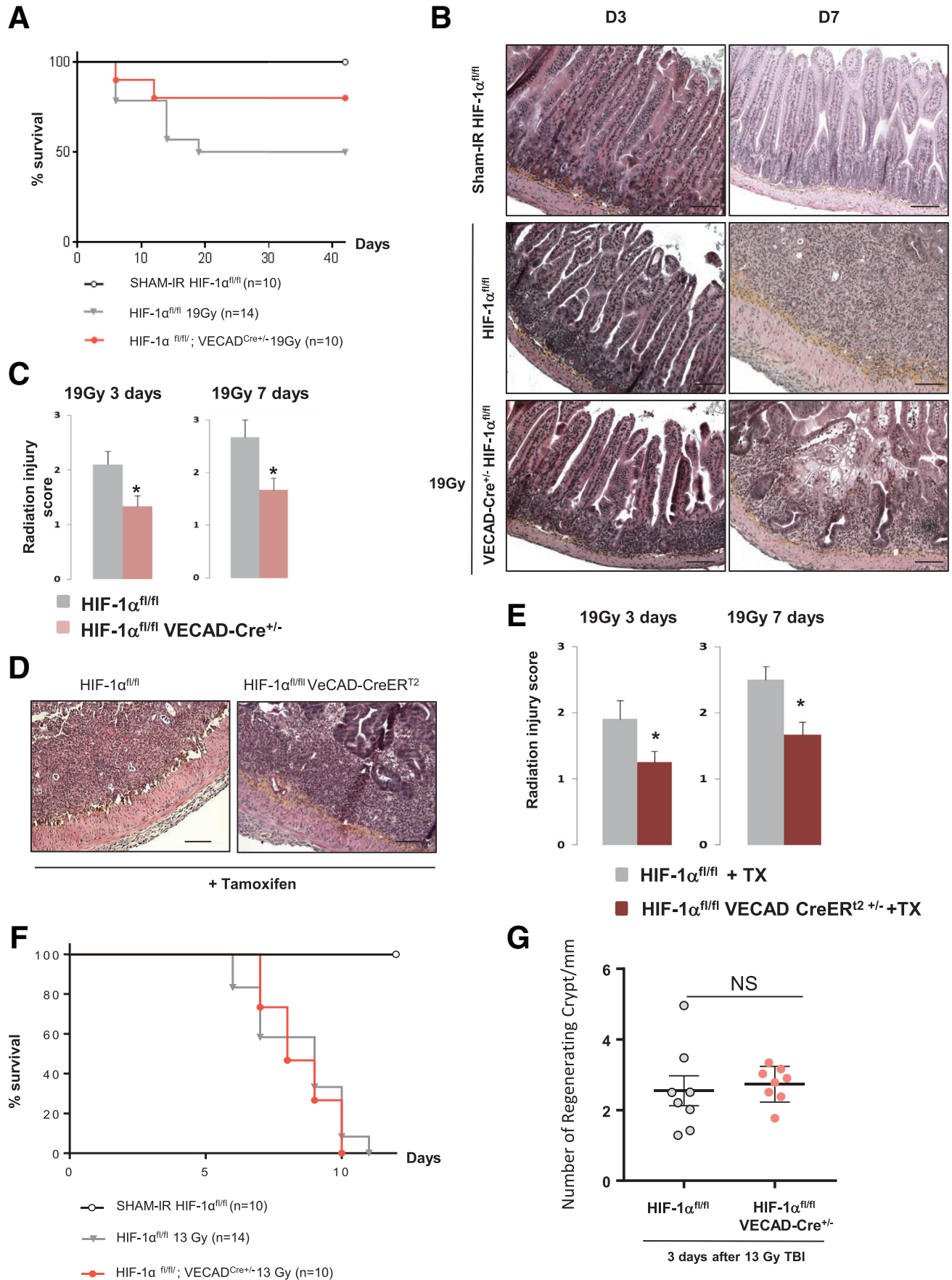


**Figure 3.** (A) Kaplan-Meier analyses representing the percent survival of irradiated HIF-1 $\alpha^{FL/FL}$  and HIF-1 $\alpha^{FL/FL}$ Villin-Cre $^{+/-}$  mice after 19-Gy localized intestinal radiation exposure. (B) Representative microscopic alterations obtained in HIF-1 $\alpha^{FL/FL}$  and in HIF-1 $\alpha^{FL/FL}$ Villin-Cre $^{+/-}$  mice 3 and 7 days after irradiation. Slides were stained with hematoxylin-eosin-saffron. Scale bar = 100  $\mu$ m. (C) Radiation injury score in HIF-1 $\alpha^{FL/FL}$  and in HIF-1 $\alpha^{FL/FL}$ Villin-Cre $^{+/-}$  mice 3 and 7 days after irradiation (n = 8–10 mice per group). (D) Radiation injury score in HIF-1 $\alpha^{FL/FL}$  and in HIF-1 $\alpha^{FL/FL}$ Villin-CreERT2 $^{+/-}$  mice treated with tamoxifen 3 and 7 days after irradiation (n = 6–8 mice per group). (E) Kaplan-Meier analyses representing the percent survival of irradiated HIF-1 $\alpha^{FL/FL}$  and HIF-1 $\alpha^{FL/FL}$ Villin-Cre $^{+/-}$  mice after 13-Gy total body irradiation (NS,  $P = .0513$ ). NS, not significant.

performed on 5- $\mu$ m sections. For CD68 and pimonidazole immunostaining, tissue sections were heated in a citrate buffer, pH 6.0 antigen retrieval solution (Dako, Les Ulis, France) that unmasks antigens before immunostaining. Then, sections were permeabilized with a PBS-0.1% Triton-0.1% sodium citrate solution for 10 minutes and nonspecific sites were blocked in block solution (Dako). Sections were then incubated with rabbit antimouse CD68 from Abcam (Paris, France) 1/200° or antipimonidazole (Hypoxyprobe-1 kit) 1/200 for 1 hour at room temperature. Negative control animals were not exposed to primary antibodies. All samples were incubated with an antirabbit-HRP (Dako) for 45 minutes. For staining and counterstaining procedures,

Histogreen (Eurobio/Abcys, Courtaboeuf, France), nuclear fast red, and Hemalun (Sigma) were used according to the manufacturer's instructions.

For the CD68 infiltration score, the number of CD68 $^{+}$  cells related to a fixed area was determined using Histolab software (Micorvision Instruments, Evry, France). For BS-1 lectin visualization, intestinal tissues were embedded with Tissue-Tek OCT mounting medium and frozen in isopentane cooled by liquid nitrogen. Frozen sections of 30  $\mu$ m were fixed using 4% paraformaldehyde for 10 minutes and nuclei were counterstained with Dapi according to the manufacturer's instructions. Z-stack images were recorded using a Zeiss LSM 780 confocal microscope (Zeiss France, Marly Le Roi, France).





### Human Rectal Tissues

Human rectal tissues were obtained at the Department of Pathology, Gustave Roussy Institute (Villejuif, France) following institutional ethical guidelines and French Medical Research Council guidelines. Tissue specimens from 12 patients treated for rectal adenocarcinoma with preoperative radiotherapy were included. HIF-1 $\alpha$  labeling was performed by routine immunohistology using the rabbit anti HIF-1 $\alpha$  antibody (Abcam).

### Total RNA Isolation, Reverse Transcription, Real-Time PCR, and Taqman Low-Density Array

Total RNA from whole intestinal tissue was prepared with the total RNA isolation kit (Rneasy Mini Kit, Qiagen, Valencia, CA). After quantification on a NanoDrop ND-1000 apparatus (NanoDrop Technologies, Rockland, DE), 1  $\mu$ g of RNA was used for reverse transcription with the High-Capacity Reverse Transcription Kit (Applied Biosystems, Courtaboeuf, France) according to the manufacturer's instructions. Predeveloped TaqMan Gene Expression Assays and TaqMan Mouse Immune Array (Applied Biosystems) were used according to the manufacturer's instructions. PCR was performed with the ABI PRISM 7900 Sequence detection system (Applied Biosystems). Analyses were conducted according to the following procedure previously described in detail.<sup>19</sup> Briefly, Ct values were extracted from a global analysis using RQ Manager software (Applied Biosystems) to apply and normalize optimal baselines and threshold parameters for each target. Data Assist software was then used to determine fold changes, with fixed criteria: a maximum allowable Ct value at 37 was fixed and maximum Ct values were not included in calculations. For all analyses, the reference sample group was the Sham-IR group, automatically leading the mean of the reference group to the value 1. Normalization was performed using a global normalization method: the software first finds the common assays among all samples and then uses the median CT of those assays as the normalizer, on a per sample basis.<sup>20</sup> *P* values were adjusted using the Benjamini-Hochberg false discovery rate method. Volcano plots were created and used to select the differentially expressed genes using a fold change cutoff of 1.5 and adjusted *P* < .05. For unsupervised hierarchical clustering analyses and heat map creation, distances between samples were calculated for hierarchical clustering based on the  $\Delta$ CT values using Pearson's correlation, assay centric as map type, and average linkage as clustering method.

For *in vitro* experiments, real-time PCR for mRNA expression was performed using individual predeveloped TaqMan Gene Expression Assays (Applied Biosystems).

### In vitro RNA Interference of HIF-1 $\alpha$

Primary human intestinal microvascular endothelial cells (HIMECs) were prepared as described.<sup>21,22</sup> HIMECs (passage 4) and human umbilical vein endothelial cells (HUVECs) (passage 3) were transfected as described previously.<sup>23</sup> Briefly, cells were seeded into 6-well plates for 48 hours to reach 50%–70% confluence and were transfected with siRNA (100 nM) using Dharmafect according to the manufacturer's protocols (Dharmacon, Chicago, IL). The antibiotic-free medium was replaced 48 hours after transfection and cells were irradiated and processed 4 days postirradiation for real-time PCR. Human siRNA and nontargeting negative control siRNA (ON-TARGETplus SMART-pool HIF1A L-004018-00, and ON-TARGETplus Nontargeting Pool) were from Dharmacon (Chicago, IL). Knockdown efficiency was measured by real-time PCR.

### Analysis of Rolling and Adhesion by Intravital Microscopy

Intravital microscopy was performed using a Nikon Eclipse TE300 inverted microscope interfaced with a high-speed, high-sensitivity CCD camera Rolera em-c<sup>2</sup> (QImaging, Canada). Briefly, mice were anesthetized using ketamine/xylazine (1/10 ratio), whole blood cells were labeled after an intravenous retro-orbital injection of 50  $\mu$ L of 1 mg/mL rhodamine solution (Sigma) and the mesentery was externalized. Five minutes after the injection, a mesenteric venule of about 150  $\mu$ m diameter was placed on the microscope ( $\times$ 20 objective) and the acquisition was recorded for 5 minutes using the MetaVue Imaging software (Molecular Devices, Sunnyvale CA). For each mouse, between 3 and 5 movies were recorded. Analyses were performed using Imaris software (Bitplane, Switzerland) using a standardized process and parameters were applied for all mice. The speed of each event (object detected using Imaris software) was automatically calculated. For each movie we obtained a mean of 10,000 events associated with a speed between 0 and 1000  $\mu$ m/s. GraphPad Prism software (La Jolla, CA) was used to calculate event frequency distribution according to the speed, and results were normalized to the number of events for each movie. Results presented are the means of 3 movies per mouse.

**Figure 4.** (See previous page). (A) Kaplan-Meier analyses representing the percent survival of irradiated HIF-1 $\alpha$ <sup>FL/FL</sup> and HIF-1 $\alpha$ <sup>FL/FL</sup>VEcad<sup>Cre+/-</sup> mice after 19-Gy localized intestinal radiation exposure. (B) Representative microscopic alterations obtained in HIF-1 $\alpha$ <sup>FL/FL</sup> and in HIF-1 $\alpha$ <sup>FL/FL</sup>VEcad<sup>Cre+/-</sup> mice 3 and 7 days after irradiation. Slides were stained with hematoxylin-eosin-saffron. Scale bar = 100  $\mu$ m. (C) Radiation injury score in HIF-1 $\alpha$ <sup>FL/FL</sup> and in HIF-1 $\alpha$ <sup>FL/FL</sup>VEcad<sup>Cre+/-</sup> mice 3 and 7 days after irradiation (*n* = 10–12 mice per group). \**P* < .05 versus HIF-1 $\alpha$ <sup>FL/FL</sup> irradiated group. (D) Representative microscopic alterations obtained in HIF-1 $\alpha$ <sup>FL/FL</sup> and in HIF-1 $\alpha$ <sup>FL/FL</sup>VEcad<sup>CreER<sup>2</sup>+/-</sup> mice previously injected with tamoxifen at 3 and 7 days after irradiation. Slides were stained with hematoxylin-eosin-saffron. Scale bar = 100  $\mu$ m. (E) Radiation injury score in each group (*n* = 8 mice per group). \**P* < .05 versus HIF-1 $\alpha$ <sup>FL/FL</sup> + tamoxifen irradiated group. (F) Kaplan-Meier analyses representing the percent survival of irradiated HIF-1 $\alpha$ <sup>FL/FL</sup> and HIF-1 $\alpha$ <sup>FL/FL</sup>VEcad<sup>Cre+/-</sup> mice after 13-Gy total body irradiation. (G) Level of regenerating crypts in irradiated HIF-1 $\alpha$ <sup>FL/FL</sup> and HIF-1 $\alpha$ <sup>FL/FL</sup>VEcad<sup>Cre+/-</sup> mice 3 days after 13-Gy total body irradiation.



## Statistical Analysis

Data are given as means  $\pm$  standard error of the mean. Statistical analyses were performed by analysis of variance or with Student *t* test with a level of significance of  $P < .05$ . Mouse survival curves were calculated by the Kaplan-Meier method and compared using the log-rank test.

## Results

### *Epithelial HIF1 $\alpha$ Deletion Does Not Alter Radiation-Induced Intestinal Injury*

HIF-1 $\alpha$  immunostaining in human rectum or in murine intestinal tissue revealed that HIF-1 $\alpha$  is mainly expressed in epithelial and endothelial cells (Figure 2). To study the consequences of genetic inactivation of HIF-1 $\alpha$  in endothelial cells and in epithelial cells, we crossed HIF-1 $\alpha$  floxed mice (HIF-1 $\alpha^{F1/FL}$ ) with VECad-Cre, VECad-CreER<sup>T2</sup>, Villin-Cre, or Villin-CreER<sup>T2</sup> mice to produce constitutive or inducible endothelial- or epithelial-specific HIF-1 $\alpha$  knockout mice (Figure 1A–C). The specificity of endothelium or epithelium recombination events in intestinal tissue was evaluated using ROSA26 reporter mice crossed with each Cre mouse strain (Figure 1D). By monitoring HIF-1 $\alpha$  mRNA expression in intestinal tissue in HIF-1 $\alpha^{F1/FL}$ VECad-Cre<sup>+/-</sup> mice or HIF-1 $\alpha^{F1/FL}$ Villin-Cre<sup>+/-</sup> mice, we observed decreased expression of HIF-1 $\alpha$  mRNA only in HIF-1 $\alpha^{F1/FL}$  Villin-Cre<sup>+/-</sup> mice compared with HIF-1 $\alpha^{F1/FL}$  mice, confirming the fact that HIF-1 $\alpha$  is mainly expressed in the epithelium (Figure 1E). Based on this observation, we hypothesized that specific HIF-1 $\alpha$  deletion in epithelium could have a significant impact on intestinal radiation injury. We monitored the survival of HIF-1 $\alpha^{F1/FL}$  or HIF-1 $\alpha^{F1/FL}$  Villin-Cre<sup>+/-</sup> mice in both a model of radiation enteropathy after localized intestinal radiation exposure at 19 Gy or in a model of gastrointestinal syndrome after TBI at 13 Gy. Surprisingly, we did not observe differences in survival after either focal irradiation (Figure 3A) or TBI (Figure 3E). We examined intestinal tissue injury 3 and 7 days postirradiation in the model of radiation enteropathy and no differences in the radiation injury score were observed, regardless of HIF-1 $\alpha$  expression in the epithelium (Figure 3B and C). Interestingly, we confirmed these results in a model of tamoxifen-inducible HIF-1 $\alpha$  deletion in epithelium. No differences were observed in the radiation injury score for irradiated HIF-1 $\alpha^{F1/FL}$ Villin-CreER<sup>T2+/-</sup> mice or for HIF-1 $\alpha^{F1/FL}$  mice treated with tamoxifen (Figure 3D).

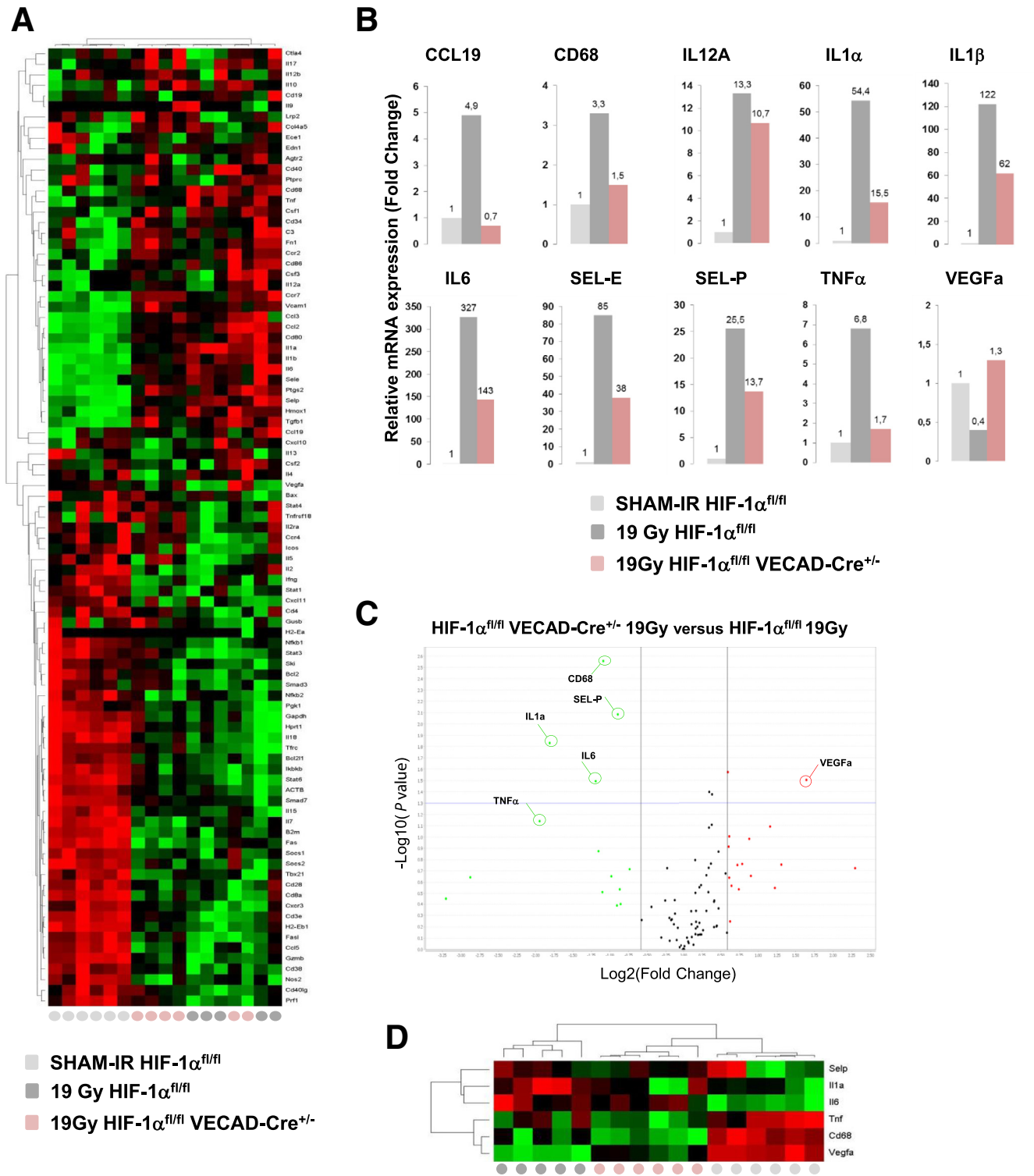
### *Constitutive and Inducible Endothelial HIF1 $\alpha$ Deletion Protects Against Radiation-Induced Enteropathy, but Not Against Gastrointestinal Syndrome*

We next evaluated the effects of endothelial HIF-1 $\alpha$  deletion on radiation-induced enteritis. Survival analyses revealed that about 50% of irradiated HIF-1 $\alpha^{F1/FL}$  mice died ( $P = .009$  vs Sham-IR HIF-1 $\alpha^{F1/FL}$  mice), whereas 80% of irradiated HIF-1 $\alpha^{F1/FL}$ VECad-Cre<sup>+/-</sup> mice were alive 6 weeks after irradiation (NS  $P = .132$  vs Sham-IR HIF-1 $\alpha^{F1/FL}$  mice) (Figure 4A).

At tissue level, irradiated HIF-1 $\alpha^{F1/FL}$ VECad-Cre<sup>+/-</sup> mice exhibited reduced acute enteritis severity 3 and 7 days after irradiation compared with irradiated HIF-1 $\alpha^{F1/FL}$  mice (Figure 4B and C). The protective effect of HIF-1 $\alpha$  endothelial deletion was confirmed in tamoxifen-inducible mice. At both 3 days and 7 days after irradiation, radiation injury score was reduced in irradiated HIF-1 $\alpha^{F1/FL}$ VECad-CreER<sup>T2+/-</sup> mice compared with irradiated HIF-1 $\alpha^{F1/FL}$  mice treated with tamoxifen (Figure 4D and E). Interestingly, we did not observe any protective effect of endothelial HIF-1 $\alpha$  deletion after 13 Gy TBI in the 2 mouse strains, which had the same survival rates and showed no difference in regenerating crypt numbers 3 days after radiation exposure (Figure 4F and G).

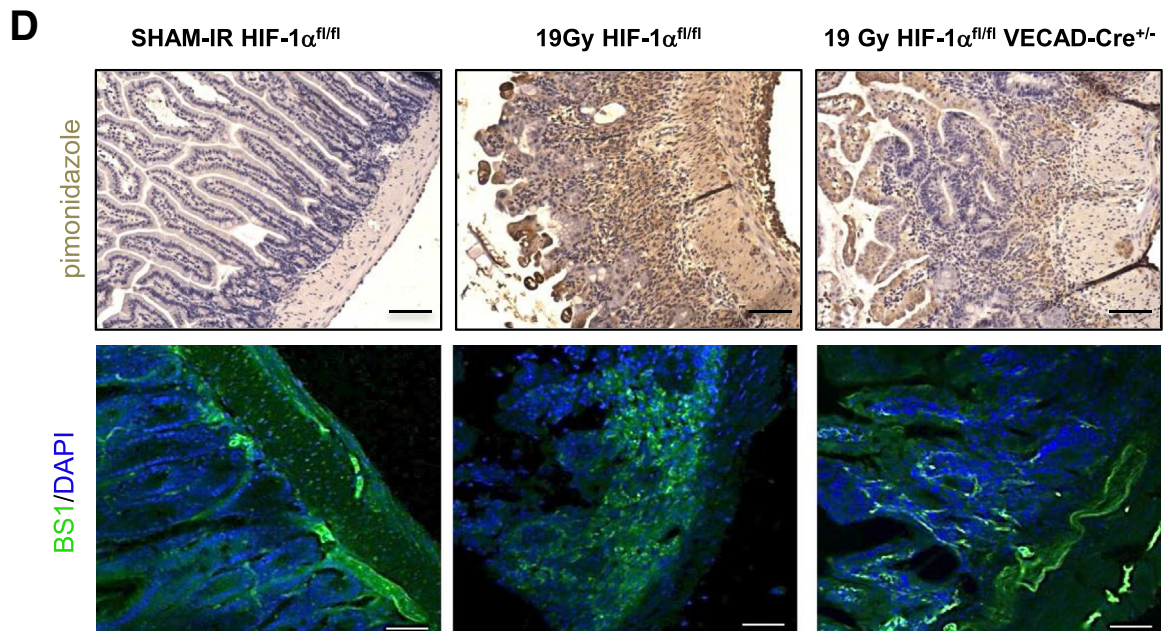
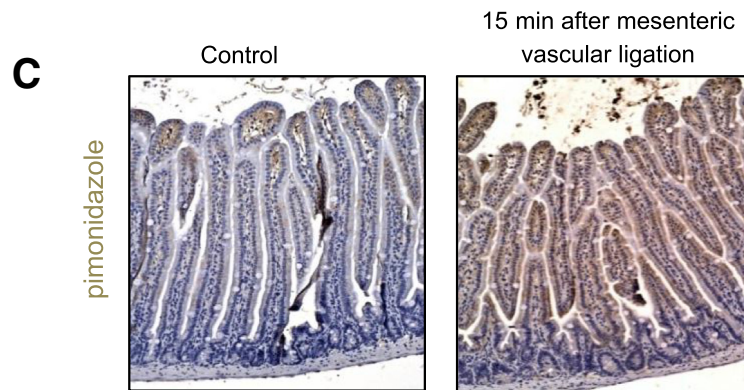
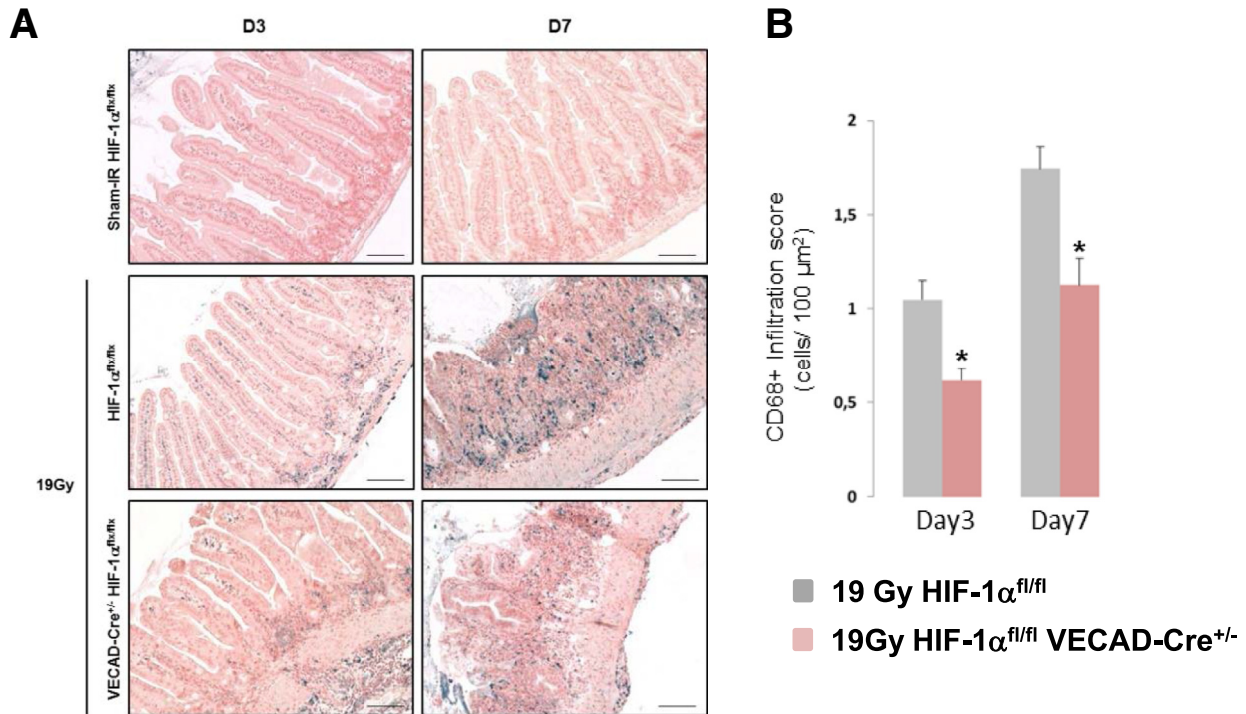
### *Constitutive Endothelial HIF-1 $\alpha$ Limits the Intestinal Radiation-Induced Molecular Inflammatory Response, Tissue Hypoxia, and Vascular Injury*

A molecular profile was obtained 7 days after irradiation on whole tissue using real-time PCR and Taqman Low Density Array cards. Hierarchical clustering analyses discriminated Sham-IR from irradiated mice, but not according to the expression of HIF-1 $\alpha$  in endothelial cells (Figure 5A). However, in-depth data analyses showed that, for a panel of genes, the level of radiation-induced molecular response was lower in HIF-1 $\alpha^{F1/FL}$ VECad-Cre<sup>+/-</sup> mice than in HIF-1 $\alpha^{F1/FL}$  mice. Radiation-induced up-regulation of proinflammatory cytokines/chemokines CCL19, interleukin (IL)12A, IL1 $\alpha$ , IL1 $\beta$ , IL6, E- and P-selectins, and tumor necrosis factor- $\alpha$  was more pronounced in HIF-1 $\alpha^{F1/FL}$  mice than in HIF-1 $\alpha^{F1/FL}$ VECad-Cre<sup>+/-</sup> mice (Figure 5B). Interestingly, volcano plots confirmed differences between the molecular responses of irradiated HIF-1 $\alpha^{F1/FL}$  and HIF-1 $\alpha^{F1/FL}$  VECad-Cre<sup>+/-</sup> mice and, using unsupervised hierarchical clustering analyses, a panel of 6 genes was able to discriminate irradiated groups according to their genotype (Figure 5C and D). In the volcano plot, the highest *P* value was linked to CD68, a glycoprotein expressed in various cells of the macrophage lineage. Immunolabeling of CD68 in intestinal tissues showed that HIF-1 $\alpha$  deletion in endothelium limits radiation-induced macrophage infiltration (Figure 6A and B). Interestingly, molecular analyses also revealed that expression of VEGFA was reduced in irradiated HIF-1 $\alpha^{F1/FL}$  mice, but not in HIF-1 $\alpha^{F1/FL}$ VECad-Cre<sup>+/-</sup> mice, suggesting effects on hypoxia and vascular integrity. We then monitored tissue hypoxia using the hypoxia-probe pimonidazole hydrochloride. We checked immunolabeling specificity in a positive control generating tissue hypoxia after 15 minutes of mesenteric vascular ligation (Figure 6C). After intravenous pimonidazole injection and immunolabeling, radiation exposure induced acute intestinal hypoxia 7 days after irradiation and HIF-1 $\alpha$  deletion was associated with reduced hypoxia (Figure 6D). BS1-lectin injection showed that hypoxia areas were associated with altered microvasculature and a preserved vascular integrity was observed in irradiated HIF-1 $\alpha^{F1/FL}$ VECad-Cre<sup>+/-</sup> mice compared with irradiated HIF-1 $\alpha^{F1/FL}$  mice (Figure 6D). To



**Figure 5. (A)** Differential expression of inflammation/immune-related genes in the mouse intestine 7 days after irradiation. Hierarchical clustering analyses were performed and the results were visualized in the heat map. **(B)** Individual fold change determined for a panel of genes demonstrating a reduced inflammatory response in the irradiated HIF-1 $\alpha^{FL/FL}$  group compared with the HIF-1 $\alpha^{FL/FL}$  VECad-Cre $^{+/-}$  group. **(C)** Volcano plot analyses between the irradiated HIF-1 $\alpha^{FL/FL}$  group and the irradiated HIF-1 $\alpha^{FL/FL}$  VECad-Cre $^{+/-}$  group (fixed fold change 1.5 and  $P = .05$ ). **(D)** Hierarchical clustering analyses were performed and a heat map was generated with 6 molecular entities. SEL-P, Selectin-P; TNF, tumor necrosis factor; VEGF, vascular endothelial growth factor.





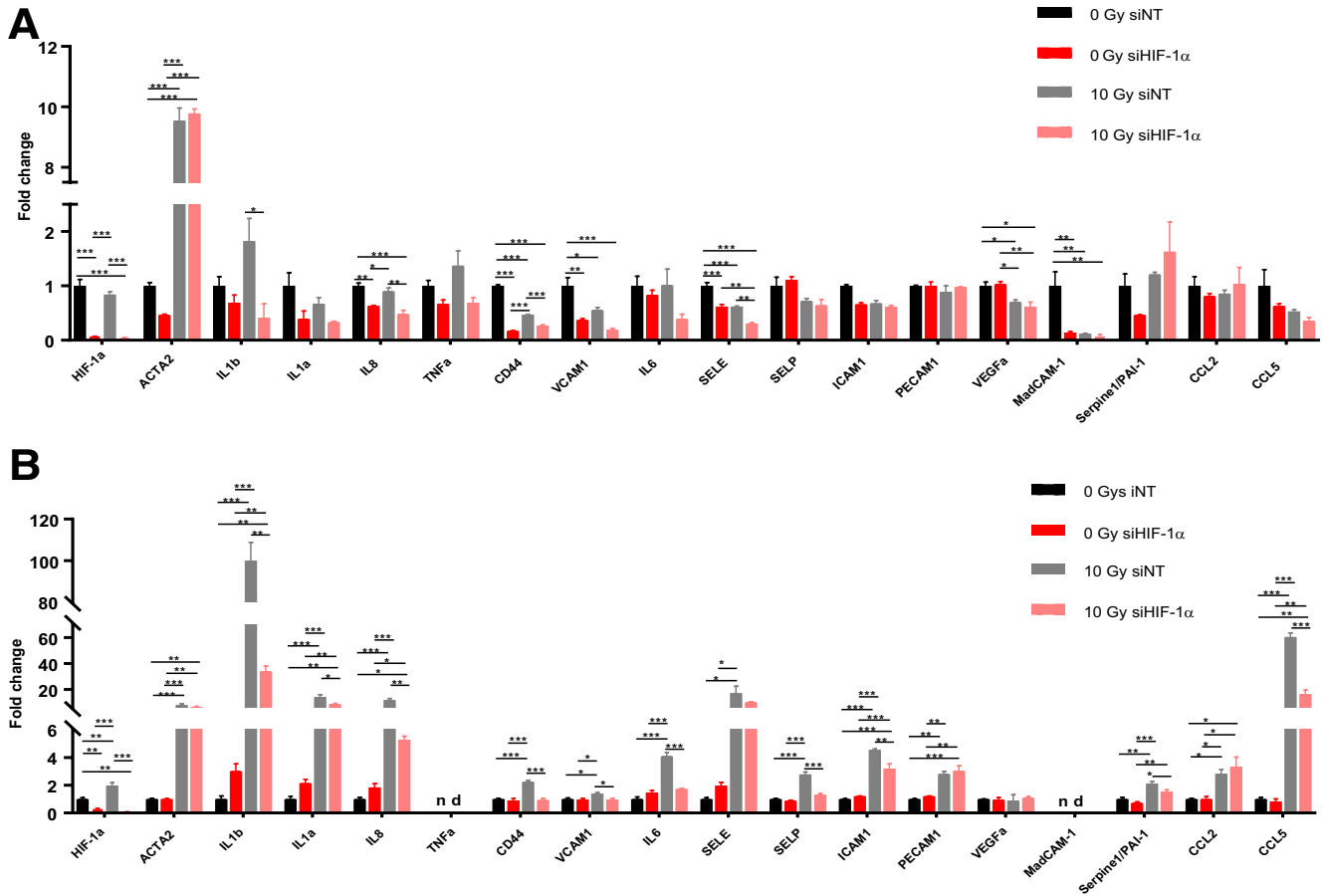


**Figure 7. (A) HIMECs were transfected for 48 hours with nontargeting siRNA or siRNA targeting HIF-1 $\alpha$  and exposed or not to 10-Gy irradiation. mRNA expression levels of a panel of genes involved in the proinflammatory state of endothelial cells were measured 4 days after irradiation. (B) The same experiment was conducted in HUVECs. Experiments were done in triplicate and results are  $\pm$  standard error of the mean (error bars). \* $P < .05$ , \*\* $P < .01$ , and \*\*\* $P < .001$  using a 1-way analysis of variance with posttest (Tukey-Kramer multiple comparisons test). nd, not detected.**

explore whether HIF-1 $\alpha$  expression directly impacts the proinflammatory transcriptional profile of endothelial cells, HIMECs and HUVECs were knockdown for HIF-1 $\alpha$  using siRNA (Figure 7A and B). A strong silencing efficiency for both cell types was observed 2 days after transfection (ie, 91% for HIMECs and 94% for HUVECs, data not shown). In HIMECs, HIF-1 $\alpha$  knockdown reduces basal expression of IL8, CD44, E-selectin, and vascular cell adhesion molecule-1. Four days after 10-Gy irradiation, HIF-1 $\alpha$  silencing was strongly maintained and was associated with reduced expression of IL1 $\beta$ , IL8, CD44, and E-selectin, compared with irradiated cells transfected with nontargeting siRNA (Figure 7A). In HUVECs, HIF-1 $\alpha$  knockdown has no effect on basal expression of selected genes but

strongly limits the radiation-induced up-regulation of most of them including IL1 $\beta$ , IL1 $\alpha$ , IL8, IL6, CD44, P-selectin, vascular cell adhesion molecule-1, intercellular adhesion molecule-1, plasminogen activator inhibitor type-1 (PAI-1), and CCL5 (Figure 7B). Altogether, these results show that HIF-1 $\alpha$  silencing reduces the proinflammatory transcriptional profile of endothelial cells.

### *Constitutive Endothelial HIF-1 $\alpha$ Limits Interactions Between Endothelium and Blood Cells After Irradiation*

To investigate whether HIF-1 $\alpha$  impacts vascular function related to inflammatory processes, we evaluated

**Figure 6. (See previous page). (A) Representative labeling of macrophages in intestinal tissue 3 and 7 days after irradiation. Slides were stained with antibody against CD68 (blue) and counterstained with nuclear fast red (pink). Scale bar = 100  $\mu$ m. (B) Macrophage scoring (CD68<sup>+</sup> cells/area) in irradiated HIF-1 $\alpha$ <sup>FL/FL</sup> and HIF-1 $\alpha$ <sup>FL/FL</sup>VEcad<sup>Cre+/-</sup> mice after 19-Gy localized intestinal radiation exposure (n = 8–10 mice per group). \* $P < .05$  versus irradiated floxed mice for each time. (C) Representative pimonidazole immunolabeling in tissues taken after a 15-minute period of ischemia following a mesenteric ligation. (D) Representative pimonidazole immunolabeling and BS1-lectin counterstained with DAPI localization in SHAM-IR-HIF-1 $\alpha$ <sup>FL/FL</sup> and in irradiated HIF-1 $\alpha$ <sup>FL/FL</sup> or HIF-1 $\alpha$ <sup>FL/FL</sup>VEcad-Cre<sup>+/-</sup> mice 7 days after irradiation. n = 6 mice per group. Scale bar = 100  $\mu$ m.**



interactions between endothelial cells and blood cells *in vivo* by intravital microscopy. Twenty-four hours after irradiation at 19 Gy, the frequency of blood cells with a reduced velocity (including leucocytes and platelets) increased after irradiation in HIF-1 $\alpha^{FL/FL}$  mice compared with nonirradiated HIF-1 $\alpha^{FL/FL}$  mice (Figure 8A and B). These results show that irradiation stimulates blood cell/endothelium interactions, the first step before transmigration of immune cells and tissue inflammation. Although a tendency was observed for global interactions in irradiated HIF-1 $\alpha^{FL/FL}$ VECad-Cre $^{+/-}$  mice compared with nonirradiated HIF-1 $\alpha^{FL/FL}$ VECad-Cre $^{+/-}$  mice (Figure 8C), no differences were observed for the strongest interactions (ie, lowest velocity <40  $\mu$ m/s) (Figure 8D). If we focused for events of velocity <5  $\mu$ m/s (green area in Figure 8A and C), which includes firm adhesion events, we found that irradiation stimulated firm adhesion in HIF-1 $\alpha^{FL/FL}$  mice, but not in HIF-1 $\alpha^{FL/FL}$ VECad-Cre $^{+/-}$  mice. Altogether, these results corroborate the reduced intestinal injury and inflammation observed in HIF-1 $\alpha^{FL/FL}$ VECad-Cre $^{+/-}$  mice compared with HIF-1 $\alpha^{FL/FL}$  mice.

## Discussion

Whereas the role of hypoxia in the radiation response of tumors has been previously investigated,<sup>24</sup> the hypoxia-dependent molecular mechanisms of the normal tissue response remain poorly understood. A first report, by Vujaskovic et al<sup>25</sup> showed that hypoxia contributes to normal tissue injury in a model of radiation-induced lung injury in rats. To our knowledge, no information is available concerning hypoxia-dependent molecular mechanisms in radiation-induced enteritis. In this work we provide *in vivo* evidence that HIF-1 $\alpha$  impacts radiation-induced intestinal injury and that this role differs according to the targeted cell type. The relative contribution of endothelial and epithelial compartments to bowel radiation injury is still debated and the results presented here support the concept that endothelium-dependent mechanisms contribute actively to the initiation of radiation-induced injury in normal tissue.

We first hypothesized that HIF-1 $\alpha$  deletion in epithelial cells could impact the intestinal response following radiation exposure. We had 3 arguments justifying explore this hypothesis: (1) the gastrointestinal tract is able to adapt to

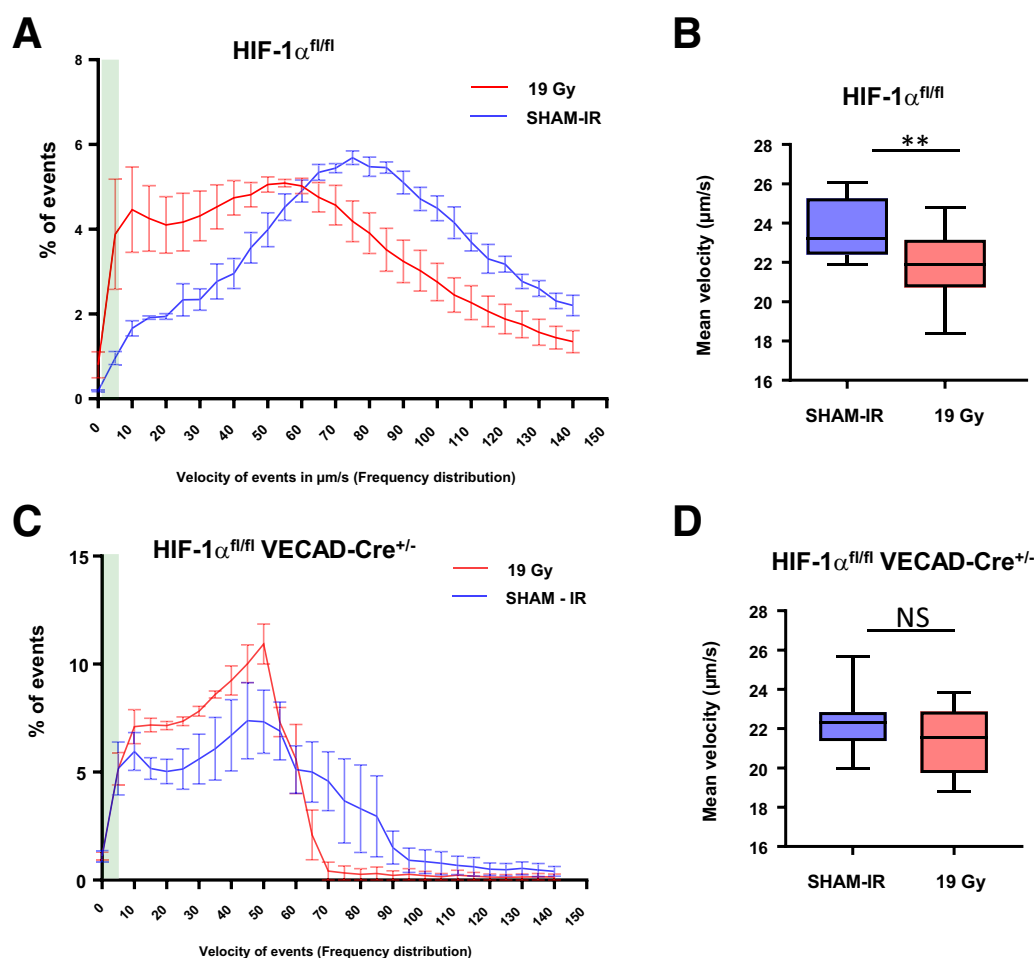


**Figure 8.** (A) Speed ( $\mu$ m/s) of event frequency distribution (in percent) in control and irradiated HIF-1 $\alpha^{FL/FL}$  mice. (B) Mean velocity in  $\mu$ m/s of events with a speed <40  $\mu$ m/s in control and irradiated HIF-1 $\alpha^{FL/FL}$  mice. (C) Speed ( $\mu$ m/s) of event frequency distribution (in percent) in control and irradiated HIF-1 $\alpha^{FL/FL}$  VECad-Cre $^{+/-}$  mice. (D) Mean velocity in  $\mu$ m/s of events with a speed <40  $\mu$ m/s in control and irradiated HIF-1 $\alpha^{FL/FL}$  VECad-Cre $^{+/-}$  mice. n = 4 mice per group.

significant changes in tissue oxygen availability,<sup>26</sup> (2) HIF-1 $\alpha$  triggers the transcription of genes involved in epithelium integrity,<sup>27</sup> and (3) HIF-1 $\alpha$  is mainly expressed in epithelial cells. Surprisingly, we found that constitutive or inducible epithelial HIF-1 $\alpha$  deletion does not influence radiation-induced intestinal acute injury after either localized or TBI irradiation. There are conflicting results in the literature concerning the role of HIF-1 in intestinal inflammation. Using FABP promoter-driven Cre recombinase mice, Karhausen et al<sup>28</sup> showed that specific epithelial constitutive repression of HIF-1 $\alpha$  resulted in more severe 2,4,6-trinitrobenzene sulfonic acid-induced colitis, whereas constitutive epithelial HIF-1 overexpression was protective. Paradoxically, using Villin-Cre mice, it was shown that chronically increased HIF signaling in epithelial cells augments inflammation in a Dextran Sulfate Sodium-induced colitis model<sup>29</sup> and that HIF-1 $\alpha$  deletion reduces inflammation in a model of sulindac-induced colon injury.<sup>30</sup> It is not clear whether model-dependent results are caused by the stress-induced inflammatory process or by the specific Cre recombinase mice used to produce cell-specific deletion of HIF signaling. It was reported that, using ROSA26R LacZ reporter mice crossed with FABP-Cre mice, recombination efficiency was approximately 60% in epithelial cells, whereas using Villin-Cre mice recombination efficiency was complete.<sup>29</sup> Using Villin-Cre mice, we confirmed that recombination efficiency is complete in epithelium, suggesting that the conflicting results previously cited and our findings are probably caused by the specificity of the stress induced inflammatory insult (Dextran Sulfate Sodium, 2,4,6-trinitrobenzene sulfonic acid, or ionizing radiation exposure) more than Cre mouse models used to produce specific deletion. Mucosal inflammation is largely controlled by nonepithelial cells, including Paneth cells, leucocytes, smooth muscle cells, and endothelial cells.<sup>31,32</sup> It has been previously reported that the same protein could play different roles according to its expression in epithelial or endothelial cells. Ishikawa et al<sup>33</sup> produced myeloid-, epithelium-, or endothelium-specific cyclooxygenase-2 knockout mice using, respectively, LysM, Villin, or VECad promoter driven Cre mice. In a model of Dextran Sulfate Sodium-induced inflammation, colitis was exacerbated when Cox2 was deleted in myeloid or endothelial lineages, but not in the epithelial lineage. These results suggest that endothelial but not epithelial cyclooxygenase-2 expression is important for epithelial integrity.

Endothelium has already been described as a crucial compartment involved in gastrointestinal syndrome, which follows total body or abdominal irradiation.<sup>34–36</sup> Moreover, the intestinal vascular microcirculation plays a decisive role in the initiation and perpetuation of the inflammatory process by regulating the migration of leucocytes into the interstitial space; by controlling coagulation; and by producing a large panel of chemokines, cytokines, and growth factors.<sup>37,38</sup> We recently demonstrated that the endothelium directly impacts the intestinal proinflammatory response following radiation exposure and progression of radiation enteritis.<sup>19</sup> Using endothelium-specific knockout mice for PAI-1, we showed *in vivo* that a modification of

endothelium phenotype affects the progression of radiation-induced enteritis after localized irradiation. Irradiated VECad-Cre<sup>+/+</sup>/PAI-1<sup>FL/FL</sup> mice exhibited reduced acute enteritis severity with a lower CD68<sup>+</sup> cell level and increased survival compared with irradiated PAI-1<sup>FL/FL</sup> mice. Hypoxia-responsive elements are present in the PAI-1 gene promoter<sup>39,40</sup> and using VECad-Cre<sup>+/+</sup>/HIF-1 $\alpha$ <sup>FL/FL</sup> mice we showed that PAI-1 overexpression is dependent on HIF-1 $\alpha$  expression in endothelium,<sup>19</sup> suggesting that a hypoxia-PAI-1 axis could be crucial in the progression of radiation-induced enteritis through the endothelial compartment. In the current work, we demonstrate that, in the endothelium, specific HIF-1 $\alpha$  deletion protects against radiation-induced enteritis. HIF-1 $\alpha$  deletion in endothelial cells is associated with reduced blood cell-endothelium interactions, a lower level of macrophages in the lesion and a limited up-regulation of proinflammatory molecules contributing to radiation-induced intestinal injury, such as IL1 $\alpha$ , IL1 $\beta$ , and IL6 and tumor necrosis factor- $\alpha$ .<sup>4,5</sup> Moreover, expressions of E- and P-selectins described as key players in radiation-induced mucosal inflammation were also limited.<sup>41,42</sup> Finally, VECad-Cre<sup>+/+</sup>/HIF-1 $\alpha$ <sup>FL/FL</sup> mice showed preserved vasculature and less hypoxia compared with irradiated control mice. At this point in time, we are unable to know if vascular integrity is caused by reduced hypoxia or if it relates to other effects associated with HIF-1 $\alpha$  deletion. Further experiments are needed to answer this question.

Interestingly, we also observed that HIF-1 $\alpha$  expression level in the endothelium has no radioprotective effect following 13-Gy TBI radiation-induced gastrointestinal syndrome. Our results are in line with previous results from Tanigushi et al<sup>12</sup> showing that lox-stop-lox-HIF-1 $\alpha$ /Tie-2 Cre mice are not protected against acute radiation syndrome following abdominal irradiation, suggesting also that the endothelial HIF-1 $\alpha$  pool is not sufficient to impact the progression of gastrointestinal syndrome. This result also suggests differences concerning intestinal wound healing after localized irradiation or after irradiation of a large volume of intestine, and highlights the precautions necessary to extrapolate a therapeutic benefit in the context of gastrointestinal syndrome or radiation enteritis (and inversely). In the same spirit, for both radiation-induced gastrointestinal syndrome and in a model of radiation enteritis, we used a single high-dose acute exposure and raised the issue of the relevance of dose fractionation in a clinical setting. A new small animal imaged-guided radiation platform allows high-precision irradiation. Verginadis et al<sup>43</sup> recently published an interesting preclinical model in mice targeting a precise region of the small intestine thanks to the implantation of a radiopaque marker detected using the cone beam CT. This type of new relevant preclinical model allows fractionation protocols without surgery and could help to (1) model radiation fractionation regimens that mimic patient protocols, (2) study pathophysiological processes involved in radiation enteritis according to the fractionation schedule, and (3) investigate putative therapeutic strategies to limit radiation-induced intestinal injury.

Contradictory results were also published concerning the protective or deleterious role of HIF-1 $\alpha$  in vascular injury

and its effects on tissue remodeling. HIF-1 deletion in the Tie2-positive lineage is associated with increased features of cardiac pathology induced by pressure overload.<sup>44</sup> Our results showed that, in our experimental conditions, endothelial HIF-1 $\alpha$  deletion is protective, in line with a recent work published by Bryant et al.<sup>45</sup> These authors demonstrated that deletion of HIF-1 $\alpha$  in vascular endothelium using VECad-Cre mice is protective against the development of pulmonary hypertension and cardiac remodeling that follows chronic hypoxia. In a similar manner, HIF-1 $\alpha$  deletion protects the vascular system in a model of lens injury.<sup>46</sup>

Recent advances concerning the role of endothelial activation in radiation-induced normal tissue injury revealed new mechanisms and opens new perspectives in terms of therapeutic strategies. Choi et al<sup>47</sup> observed an endothelial-to-mesenchymal transition (EndoMT) in radiation-induced pulmonary fibrosis in mice and humans. They showed that radiation-induced hypoxia stimulates EndoMT via a transforming growth factor- $\beta$ -RI/Smad activation dependent on HIF-1 $\alpha$ . HIF-1 $\alpha$  knockdown limits radiation-induced EndoMT in irradiated human pulmonary artery ECs and Smad2/3 phosphorylation. Moreover, the HIF-1 $\alpha$  inhibitory agent 2-methoxyestradiol limits in vivo radiation-induced EndoMT by the down-regulation of HIF-1 $\alpha$ -dependent Smad signaling activation. Along these lines, we recently reported that EndoMT occurs in human radiation proctitis and in a pre-clinical model of radiation proctitis in mice.<sup>22</sup> Activation of the canonical transforming growth factor- $\beta$ /Smad pathway contributes to radiation enteritis or proctitis driving both the expression of PAI-1 and EndoMT.<sup>18,22,48–51</sup> In light of the current work we can hypothesize that HIF-1 deletion in endothelial reduced EndoMT and consequently tissue injury. Further experiments are needed to explore the putative causal links between hypoxia, the transforming growth factor- $\beta$ /Smad pathway, and EndoMT in the radiation-induced injury model.

Hauer-Jensen et al<sup>4</sup> recently proposed that radiation enteropathy is a useful model to explore mucosal inflammation and that mechanisms involved in radiation-induced toxicity models can putatively offer a crucial advance in other types of gastrointestinal injury, such as inflammatory bowel disease (Crohn's disease, ulcerative colitis) or intestinal ischemia-related diseases. Our work provides a new role for HIF-1 $\alpha$  in endothelium-dependent mechanisms driving inflammatory processes in the gut mucosae. Finally, therapeutic strategies to modulate hypoxia or hypoxia-related molecular mechanisms are under investigation to improve tumor control<sup>24</sup> and to protect normal tissues.<sup>52</sup> Our results show that effects on normal tissues have to be taken into account in such approaches because they could also affect the benefit/risk ratio.

## References

1. Bentzen SM. Preventing or reducing late side effects of radiation therapy: radiobiology meets molecular pathology. *Nature reviews. Cancer* 2006;6:702–713.
2. Moding EJ, Kastan MB, Kirsch DG. Strategies for optimizing the response of cancer and normal tissues to radiation. *Nat Rev Drug Discov* 2013;12:526–542.
3. Andreyev HJ, Wotherspoon A, Denham JW, Hauer-Jensen M. Defining pelvic-radiation disease for the survivorship era. *Lancet Oncol* 2010;11:310–312.
4. Hauer-Jensen M, Denham JW, Andreyev HJ. Radiation enteropathy: pathogenesis, treatment and prevention. *Nat Rev Gastroenterol Hepatol* 2014;11:470–479.
5. Francois A, Milliat F, Guipaud O, Benderitter M. Inflammation and immunity in radiation damage to the gut mucosa. *Biomed Res Int* 2013;2013:123241.
6. Wang J, Boerma M, Fu Q, Hauer-Jensen M. Significance of endothelial dysfunction in the pathogenesis of early and delayed radiation enteropathy. *World J Gastroenterol* 2007;13:3047–3055.
7. Semenza GL. Hypoxia-inducible factors: mediators of cancer progression and targets for cancer therapy. *Trends Pharmacol Sci* 2012;33:207–214.
8. Manresa MC, Taylor CT. Hypoxia inducible factor (HIF) hydroxylases as regulators of intestinal epithelial barrier function. *Cell Mol Gastroenterol Hepatol* 2017;3:303–315.
9. Eltzschig HK, Carmeliet P. Hypoxia and inflammation. *N Engl J Med* 2011;364:656–665.
10. Nizet V, Johnson RS. Interdependence of hypoxic and innate immune responses. *Nat Rev Immunol* 2009;9:609–617.
11. Traub F, Schleicher S, Kirschniak A, Zieker D, Kupka S, Weinmann M, Konigsrainer A, Kratt T. Gene expression analysis in chronic postradiation proctopathy. *Int J Colorectal Dis* 2012;27:879–884.
12. Taniguchi CM, Miao YR, Diep AN, Wu C, Rankin EB, Atwood TF, Xing L, Giaccia AJ. PHD inhibition mitigates and protects against radiation-induced gastrointestinal toxicity via HIF2. *Sci Transl Med* 2014;6:236ra64.
13. Ryan HE, Poloni M, McNulty W, Elson D, Gassmann M, Arbeit JM, Johnson RS. Hypoxia-inducible factor-1 $\alpha$  is a positive factor in solid tumor growth. *Cancer Res* 2000;60:4010–4015.
14. Alva JA, Zovein AC, Monvoisin A, Murphy T, Salazar A, Harvey NL, Carmeliet P, Iruela-Arispe ML. VE-Cadherin-Cre-recombinase transgenic mouse: a tool for lineage analysis and gene deletion in endothelial cells. *Dev Dyn* 2006;235:759–767.
15. Monvoisin A, Alva JA, Hofmann JJ, Zovein AC, Lane TF, Iruela-Arispe ML. VE-cadherin-CreERT2 transgenic mouse: a model for inducible recombination in the endothelium. *Dev Dyn* 2006;235:3413–3422.
16. Pinto D, Robine S, Jaisser F, El Marjou FE, Louvard D. Regulatory sequences of the mouse villin gene that efficiently drive transgenic expression in immature and differentiated epithelial cells of small and large intestines. *J Biol Chem* 1999;274:6476–6482.
17. el Marjou F, Janssen KP, Chang BH, Li M, Hindie V, Chan L, Louvard D, Chambon P, Metzger D, Robine S. Tissue-specific and inducible Cre-mediated recombination in the gut epithelium. *Genesis* 2004;39:186–193.
18. Milliat F, Sabourin JC, Tarlet G, Holler V, Deutsch E, Buard V, Tamarat R, Atfi A, Benderitter M, Francois A. Essential role of plasminogen activator inhibitor type-1 in radiation enteropathy. *Am J Pathol* 2008;172:691–701.

19. Rannou E, Francois A, Toullec A, Guipaud O, Buard V, Tarlet G, Mintet E, Jailliet C, Iruela-Arispe ML, Benderitter M, Sabourin JC, Milliat F. In vivo evidence for an endothelium-dependent mechanism in radiation-induced normal tissue injury. *Sci Rep* 2015;5:15738.
20. Mestdagh P, Van Vlierberghe P, De Weer A, Muth D, Westermann F, Speleman F, Vandesompele J. A novel and universal method for microRNA RT-qPCR data normalization. *Genome Biol* 2009;10:R64.
21. Binion DG, West GA, Ina K, Ziats NP, Emancipator SN, Fiocchi C. Enhanced leukocyte binding by intestinal microvascular endothelial cells in inflammatory bowel disease. *Gastroenterology* 1997;112:1895–1907.
22. Mintet E, Rannou E, Buard V, West G, Guipaud O, Tarlet G, Sabourin JC, Benderitter M, Fiocchi C, Milliat F, Francois A. Identification of endothelial-to-mesenchymal transition as a potential participant in radiation proctitis. *Am J Pathol* 2015;185:2550–2562.
23. Hneino M, Blirando K, Buard V, Tarlet G, Benderitter M, Hoodless P, Francois A, Milliat F. The TG-interacting factor TGIF1 regulates stress-induced proinflammatory phenotype of endothelial cells. *J Biol Chem* 2012;287:38913–38921.
24. Hill RP, Bristow RG, Fyles A, Koritzinsky M, Milosevic M, Wouters BG. Hypoxia and predicting radiation response. *Semin Radiat Oncol* 2015;25:260–272.
25. Vujaskovic Z, Anscher MS, Feng QF, Rabbani ZN, Amin K, Samulski TS, Dewhirst MW, Haroon ZA. Radiation-induced hypoxia may perpetuate late normal tissue injury. *Int J Radiat Oncol Biol Phys* 2001;50:851–855.
26. Grenz A, Clambey E, Eltzschig HK. Hypoxia signaling during intestinal ischemia and inflammation. *Curr Opin Crit Care* 2012;18:178–185.
27. Colgan SP, Taylor CT. Hypoxia: an alarm signal during intestinal inflammation. *Nat Rev Gastroenterol Hepatol* 2010;7:281–287.
28. Karhausen J, Furuta GT, Tomaszewski JE, Johnson RS, Colgan SP, Haase VH. Epithelial hypoxia-inducible factor-1 is protective in murine experimental colitis. *J Clin Invest* 2004;114:1098–1106.
29. Shah YM, Ito S, Morimura K, Chen C, Yim SH, Haase VH, Gonzalez FJ. Hypoxia-inducible factor augments experimental colitis through an MIF-dependent inflammatory signaling cascade. *Gastroenterology* 2008;134:2036–2048, 2048 e1–3.
30. Mladenova DN, Dahlstrom JE, Tran PN, Benthani F, Bean EG, Ng I, Pangon L, Currey N, Kohonen-Corish MR. HIF1 $\alpha$  deficiency reduces inflammation in a mouse model of proximal colon cancer. *Dis Model Mech* 2015;8:1093–1103.
31. Turner JR. Intestinal mucosal barrier function in health and disease. *Nat Rev Immunol* 2009;9:799–809.
32. Rieder F, Fiocchi C. Intestinal fibrosis in IBD: a dynamic, multifactorial process. *Nat Rev Gastroenterol Hepatol* 2009;6:228–235.
33. Ishikawa TO, Oshima M, Herschman HR. Cox-2 deletion in myeloid and endothelial cells, but not in epithelial cells, exacerbates murine colitis. *Carcinogenesis* 2011;32:417–426.
34. Cho CH, Kammerer RA, Lee HJ, Steinmetz MO, Ryu YS, Lee SH, Yasunaga K, Kim KT, Kim I, Choi HH, Kim W, Kim SH, Park SK, Lee GM, Koh GY. COMP-Ang1: a designed angiopoietin-1 variant with nonleaky angiogenic activity. *Proc Natl Acad Sci U S A* 2004;101:5547–5552.
35. Paris F, Fuks Z, Kang A, Capodiceci P, Juan G, Ehleiter D, Haimovitz-Friedman A, Cordon-Cardo C, Kolesnick R. Endothelial apoptosis as the primary lesion initiating intestinal radiation damage in mice. *Science* 2001;293:293–297.
36. Rotolo J, Stancevic B, Zhang J, Hua G, Fuller J, Yin X, Haimovitz-Friedman A, Kim K, Qian M, Cardo-Vila M, Fuks Z, Pasqualini R, Arap W, Kolesnick R. Anti-ceramide antibody prevents the radiation gastrointestinal syndrome in mice. *J Clin Invest* 2012;122:1786–1790.
37. D'Alessio S, Tacconi C, Fiocchi C, Danese S. Advances in therapeutic interventions targeting the vascular and lymphatic endothelium in inflammatory bowel disease. *Curr Opin Gastroenterol* 2013;29:608–613.
38. Danese S. Role of the vascular and lymphatic endothelium in the pathogenesis of inflammatory bowel disease: “brothers in arms.” *Gut* 2011;60:998–1008.
39. Fink T, Kazlauskas A, Poellinger L, Ebbesen P, Zachar V. Identification of a tightly regulated hypoxia-response element in the promoter of human plasminogen activator inhibitor-1. *Blood* 2002;99:2077–2083.
40. Kietzmann T, Samoylenko A, Roth U, Jungermann K. Hypoxia-inducible factor-1 and hypoxia response elements mediate the induction of plasminogen activator inhibitor-1 gene expression by insulin in primary rat hepatocytes. *Blood* 2003;101:907–914.
41. Mihaescu A, Thornberg C, Santen S, Mattsson S, Jeppsson B, Thorlacius H. Radiation-induced platelet-endothelial cell interactions are mediated by P-selectin and P-selectin glycoprotein ligand-1 in the colonic microcirculation. *Surgery* 2012;151:606–611.
42. Molla M, Gironella M, Salas A, Miquel R, Perez-del-Pulgar S, Conill C, Engel P, Biete A, Pique JM, Panes J. Role of P-selectin in radiation-induced intestinal inflammatory damage. *Int J Cancer* 2001;96:99–109.
43. Verginadis II, Kanade R, Bell B, Koduri S, Ben-Josef E, Koumenis C. A novel mouse model to study image-guided, radiation-induced intestinal injury and preclinical screening of radioprotectors. *Cancer Res* 2017;77:908–917.
44. Wei H, Bedja D, Koitabashi N, Xing D, Chen J, Fox-Talbot K, Rouf R, Chen S, Steenbergen C, Harmon JW, Dietz HC, Gabrielson KL, Kass DA, Semenza GL. Endothelial expression of hypoxia-inducible factor 1 protects the murine heart and aorta from pressure overload by suppression of TGF- $\beta$  signaling. *Proc Natl Acad Sci U S A* 2012;109:E841–E850.
45. Bryant AJ, Carrick RP, McConaha ME, Jones BR, Shay SD, Moore CS, Blackwell TR, Gladson S, Penner NL, Burman A, Tanjore H, Hemnes AR, Karwandyar AK, Polosukhin VV, Talati MA, Dong HJ, Gleaves LA, Carrier EJ, Gaskill C, Scott EW, Majka SM,



- Fessel JP, Haase VH, West JD, Blackwell TS, Lawson WE. Endothelial HIF signaling regulates pulmonary fibrosis-associated pulmonary hypertension. *Am J Physiol Lung Cell Mol Physiol* 2016;310:L249–L262.
46. Huang TQ, Wang Y, Ebrahim Q, Chen Y, Cheng C, Doughman YQ, Watanabe M, Dunwoodie SL, Yang YC. Deletion of HIF-1 $\alpha$  partially rescues the abnormal hyaloid vascular system in Cited2 conditional knockout mouse eyes. *Mol Vis* 2012;18:1260–1270.
  47. Choi SH, Hong ZY, Nam JK, Lee HJ, Jang J, Yoo RJ, Lee YJ, Lee CY, Kim KH, Park S, Ji YH, Lee YS, Cho J. A hypoxia-induced vascular endothelial-to-mesenchymal transition in development of radiation-induced pulmonary fibrosis. *Clin Cancer Res* 2015;21:3716–3726.
  48. Abderrahmani R, Francois A, Buard V, Benderitter M, Sabourin JC, Crandall DL, Milliat F. Effects of pharmacological inhibition and genetic deficiency of plasminogen activator inhibitor-1 in radiation-induced intestinal injury. *Int J Radiat Oncol Biol Phys* 2009;74:942–948.
  49. Abderrahmani R, François A, Buard V, Tarlet G, Blirando K, Hneino M, Vaurijoux A, Benderitter M, Sabourin J-C, Milliat F. PAI-1-dependent endothelial cell death determines severity of radiation-induced intestinal injury. *PloS One* 2012;7:e35740.
  50. Hneino M, Francois A, Buard V, Tarlet G, Abderrahmani R, Blirando K, Hoodless PA, Benderitter M, Milliat F. The TGF- $\beta$ /Smad repressor TG-interacting factor 1 (TGIF1) plays a role in radiation-induced intestinal injury independently of a Smad signaling pathway. *PloS One* 2012;7:e35672.
  51. Milliat F, Francois A, Isoir M, Deutsch E, Tamarat R, Tarlet G, Atfi A, Validire P, Bourhis J, Sabourin JC, Benderitter M. Influence of endothelial cells on vascular smooth muscle cells phenotype after irradiation: implication in radiation-induced vascular damages. *Am J Pathol* 2006;169:1484–1495.
  52. Olcina MM, Giaccia AJ. Reducing radiation-induced gastrointestinal toxicity: the role of the PHD/HIF axis. *J Clin Invest* 2016;126:3708–3715.

---

Received January 3, 2017. Accepted August 8, 2017.

#### Correspondence

Address correspondence to: Fabien Milliat, PhD, Research Laboratory of Radiobiology and Radiopathology, Institute for Radiological Protection and Nuclear Safety, 92265 Fontenay-aux-Roses, France. e-mail: fabien.milliat@irsn.fr.

#### Acknowledgements

The authors thank the Groupe de Soutien à l'Experimentation Animale of the IRSN for their excellent technical assistance with the breeding of mice.

#### Author contributions

A.T. performed experiments, interpreted the results, and helped write the manuscript. V.B., E.R., A.F., and G.T. performed experiments and interpreted the results. A.F., O.G., S.R., and M.L.I.-A. provided material support and critically reviewed the manuscript. F.M. conceived and designed the work, wrote the manuscript, and supervised the project.

#### Conflicts of interest

The authors disclose no conflicts.

#### Funding

This work was supported by Electricité de France EDF (Groupe Gestion Projet Radioprotection) and the Institute for Radiological Protection and Nuclear Safety (ROSIRIS program).